Polyhedron 30 (2011) 106–113

Contents lists available at ScienceDirect

Polyhedron

journal homepage: www.elsevier.com/locate/poly

Synthesis, characterization, crystal structure and antimicrobial activities of new *trans N,N*-substituted macrocyclic dioxocyclam and their copper(II) and nickel(II) complexes

G. Nirmala [a], A. Kalilur Rahiman [b], S. Sreedaran [c], R. Jegadeesh [d], N. Raaman [d], V. Narayanan [a,*]

[a] Department of Inorganic Chemistry, School of Chemical Sciences, University of Madras, Guindy Campus, Chennai 600 025, India
[b] PG and Research Department of Chemistry, The New College (Autonomous), Chennai 600 014, India
[c] Department of Chemistry, Government Arts College, Udhagamandalam 643 002, India
[d] Centre for Advanced Studies in Botany, University of Madras, Guindy Campus, Chennai 600 025, India

ARTICLE INFO

Article history:
Received 4 August 2010
Accepted 29 September 2010
Available online 7 October 2010

Keywords:
Dioxocyclam
Benzoylation
Crystal structure
Catecholase activity
Hydrolysis of 4-nitrophenylphosphate
Antimicrobial activity

ABSTRACT

New *trans*-disubstituted macrocyclic ligands, 1,8-[*N,N*-bis(3-formyl-12-hydroxy-5-methyl)benzyl]-5,12-dioxo-1,4,8,11-tetraazacyclotetradecane (L^1), 1,8-[*N,N*-bis(3-formyl-12-hydroxy-5-bromo)benzyl]-5,12-dioxo-1,4,8,11-tetraazacyclotetradecane (L^2), *N,N*-bis[1,8-dibenzoyl]-5,12-dioxo-1,4,8,11-tetraazacyclotetradecane (L^3), *N,N*-bis[1,8-(2-nitrobenzoyl)]-5,12-dioxo-1,4,8,11-tetraazacyclotetradecane (L^4), and *N,N*-bis[1,8-(4-nitrobenzoyl)]-5,12-dioxo-1,4,8,11-tetraazacyclotetradecane (L^5) were synthesized. The ligands were characterized by elemental analysis, FT IR, ^{1}H NMR and mass spectrometry studies. The crystal structure of L^1 is also reported. The copper(II) and nickel(II) complexes of these ligands were prepared and characterized by elemental analysis, FT IR, UV–Vis and mass spectral studies. The cyclic voltammogram of the complexes of ligand L^{1-3} show one-electron quasi-reversible reduction wave in the region −0.65 to −1.13 V, whereas that of L^4 and L^5 show two quasi-reversible reduction peaks. Nickel(II) complexes show one electron quasi-reversible oxidation wave at a positive potential in the range +0.95 to +1.06 V. The ESR spectra of the mononuclear copper(II) complexes show four lines, characteristic of square-planar geometry with nuclear hyperfine spin 3/2. All copper(II) complexes show a normal room temperature magnetic moment value μ_{eff} 1.70–1.73 BM which is close to the spin only value of 1.73 BM. Kinetic studies on the oxidation of pyrocatechol to *o*-quinone using the copper(II) complexes as catalysts and hydrolysis of 4-nitrophenylphosphate using the copper(II) and nickel(II) complexes as catalysts were carried out. The ligands and their complexes were also screened for antimicrobial activity against Gram-positive, Gram-negative bacteria and human pathogenic fungi.

1. Introduction

Fourteen-membered cyclam (1,4,8,11-tetraazacyclotetradecane) is one of the most versatile tetraamine ligands owing to their coordination properties and their wide range of applications [1,2]. Among potential applications of the metal complexes of these ligands are the selective removal of toxic metals from waste streams radiotherapy and contrast agents for magnetic resonance imaging [3–5]. Dioxocyclams belong to a subgroup which is claimed to be a structural intermediate between oligopeptides and saturated polyamines and which has also been extensively investigated [6]. Typically, the 14-membered dioxocyclams, like porphyrins and corrin, incorporate metal ions into their cavities and form stable square planar complexes with several configurations [7,8]. Oxopolyamines have been extensively studied due to their important biological functions and some unusual properties [9,10].

It is possible to carry out the modification of tetraaza macrocyclic ligands to control and tune the redox properties of coordinated metal centres [11]. Variations can be introduced by altering the macrocyclic ring size or by placing substituents on the nitrogen donors and/or ring framework. Of these approaches, N-functionalization with four identical pendant arms is straightforward [12]. So far, great effort has been devoted to the incorporation of functionalized pendant groups into a saturated macrocyclic tetraamine structure to modify its conformational properties and the redox properties of its metal complexes [13–15].

The cyclam derivatives are also used as spacers (i.e., the bridge between the coordinating units) because of their exceptional coordination properties and the abundant available literature describing efficient and straightforward N- or C-substitution strategies [16]. The nature and redox state of the metal ions located in the

* Corresponding author. Tel./fax: +91 44 2230 0488.
E-mail address: vnnara@yahoo.co.in (V. Narayanan).

0277-5387/$ - see front matter © 2010 Elsevier Ltd. All rights reserved.
doi:10.1016/j.poly.2010.09.036

macrocyclic spacer units drastically influences their properties [17]. Gasnier et al. [18] have reported supramolecular coordination materials based on a bis-terpyridine-functionalized dioxocyclam ligand.

The chemistry of N-functionalized cyclam based compartmental ligands and their copper(II) and nickel(II) complexes remain an important field of research. Macrocyclic dioxotetraamines bearing functionalized pendant groups are powerful chelating agents, and can coordinate with many transition metal ions to form complexes which are effective oxidants and biomimetic redox catalysts [19]. However, up to now, only a few examples of such functionalized macrocyclic dioxotetraamines have been reported [20,21]. Herein, we report the synthesis and characterization of five new macrocyclic dioxocyclam ligands and their complexation properties with Cu(II) and Ni(II) as well as the crystal structure of the ligand L^1.

2. Experimental

2.1. Analytical and physical measurements

Elemental analysis of the complexes was obtained using a Haereus CHN rapid analyzer. FT IR spectra were recorded on a Shimadzu FT IR 8300 series spectrophotometer in the range 4000–400 cm^{-1} using spectral grade KBr. ^1H NMR spectra were recorded using a JEOL GSX 400 MHz NMR spectrometer. Atomic absorption spectral data were recorded using a Varian spectra AA-200 model atomic absorption spectrophotometer. FAB^+ mass spectrum was obtained on a JEOL SX102/DA-6000 Mass Spectrometer using m-nitro benzyl alcohol (NBA) as the matrix. The accelerating voltage was 10 kV and the spectrum was recorded at room temperature. Electronic spectral studies were carried out on a Hitachi 320 spectrophotometer in the range 200–1100 nm. Molar conductivity was measured by using an Elico digital conductivity bridge model CM-88 using freshly prepared solution of the complex in dimethylformamide. Cyclic voltammograms were obtained on a CHI-600A electrochemical analyzer. The measurements were carried out under oxygen-free conditions using a three-electrode cell in which a glassy carbon electrode was the working electrode, a saturated Ag/AgCl electrode was the reference electrode and platinum wire was used as the auxiliary electrode. A ferrocene/ferrocenium (1+) couple was used as an internal standard and $E_{1/2}$ of the ferrocene/ferrocenium (Fc/Fc^+) couple under the experimental condition was 470 mV. Tetra(*n*-butyl)ammonium perchlorate (TBAP) was used as the supporting electrolyte. Room temperature magnetic moments were measured on a PAR vibrating sample magnetometer Model-155. X-band EPR spectra were recorded at 25 °C on a Varian EPR-E 112 spectrometer using diphenylpicrylhydrazine (DPPH) as the reference. Catalytic oxidation of catechol to *o*-quinone by the copper complexes and hydrolysis of 4-nitrophenylphosphate by the copper and nickel complexes were studied in 10^{-3} M dimethylformamide solutions. The oxidation reactions were followed spectrophotometrically with the strongest absorption band of *o*-quinone at 390 nm and monitoring the increase in absorbance; the hydrolysis of 4-nitrophenylphosphate was monitored by following the UV absorbance change at 420 nm (assigned to the 4-nitrophenolate anion) as a function of time. A plot of log $(A_\infty/A_\infty - A_t)$ versus time was made for each complex and the rate constants for the catalytic oxidations and hydrolysis of 4-nitrophenylphosphate were calculated.

The ligand L^1 was crystallized from chloroform solution in the space group $P2_1/n$ with two half-molecules of the macrocycle and one molecule of chloroform solvent in the asymmetric unit. Light yellow crystal of the ligand L^1, 0.30 × 0.25 × 0.20 mm, was used for indexing and intensity data collection was carried out using Bruker SMART APEX-CCD diffractometer equipped with a fine focus, 3 kW sealed tube X-ray source and graphite monochromated Mo Kα radiation at 293(2) K. The data covered over a hemisphere of reciprocal space by a combination of three sets of exposures; each set had a different ø angle (0°, 88° and 180°) for the crystal and each exposure of 10 s covered 0.3° in ω. The detector was at a distance of 4 cm from the crystal and the swing angle of the detector was −35°. Cell refinement and data reduction were performed by the SMART and SAINT programs [22]. The final unit cell was obtained from xyz centroids of reflections after integration. Intensity data were corrected for Lorentz and polarization effects, scale variation, for decay and absorption: a multi scan absorption correction was applied, based on the intensities of symmetry related reflections measured at different angular settings (SADABS) and reduced to F_o^2.

The structure was solved by direct methods using the program SHELXS-97 [23], a package for crystal structure solution using direct methods. All non-hydrogen atoms were refined anisotropically [23] by full-matrix least-square procedures with the weight $w = 1/[\sigma^2(F_o^2) + (0.2000P)^2]$, where $P = (F_o^2 + 2F_o^2)/3$. Some of the hydrogen atoms were geometrically fixed and allowed to ride on the parent carbon atom and other hydrogen atoms were located from the different Fourier map and refined isotropically. The CCDC reference number is 723256. The crystallographic data and structure refinement for the ligand L^1 are given in Table S1. The selected bond lengths and angles are listed in Table S2.

2.2. Chemicals and reagents

Synthesis of the parent ligand, 1,4,8,11,-tetraazacyclotetradecane 5,12-dione, as well as 5-methyl salicylaldehyde, 3-chloromethyl-5-methyl salicylaldehyde and 3-chloromethyl-5-bromo salicylaldehyde were carried out according to literature methods [24,25]. Benzoyl chloride and nitrobenzoyl chlorides were purchased from Sigma–Aldrich and used as such. Analytical grade methanol, acetonitrile and dimethylformamide were purchased from Qualigens and used as such. TBAP was used as supporting electrolyte in electrochemical measurement was purchased from Fluka and recrystallised from hot methanol. (**Caution!** TBAP is potentially explosive; hence care should be taken in handling the compound). All other chemicals and solvents were of analytical grade and were used as received without any further purification.

2.3. Synthesis of the ligands

2.3.1. Synthesis of 1,8-[N,N-bis(3-formyl-12-hydroxy-5-methyl)-benzyl]-5,12-dioxo-1,4,8,11-tetraazacyclotetradecane (L^1)

Two equivalent of 3-chloromethyl-5-methyl salicylaldehyde (1.47 g, 0.008 mol) in 50 mL of acetonitrile was rapidly added to 5,12-dioxo-1,4,8,11-tetraazacyclotetradecane (1 g, 0.004 mol) dissolved in 50 mL of hot acetonitrile and stirred for 24 h. The yellow precipitate obtained was filtered, washed with small quantity of acetonitrile and dried under vacuum. This was recrystallized from water to afford L^1 as a yellowish white solid.

Yield: 1.72 g (75 %) M.p: 300 °C. *Anal.* Calc. for $[C_{28}H_{34}O_6N_4]$: C, 64.33; H, 6.56; N, 10.70. Found: C, 64.23; H, 6.47; N, 10.60%; Selected IR (KBr) (ν/cm^{-1}): 3398 ν(OH), 3289 ν(NH), 1670, 1648 ν(C=O). 1H NMR (δ ppm in $CDCl_3$): 1.17 (s, 6H, CH_3), 1.9–2.26 (m, 12H, α-CH_2), 3.35–3.43 (m, 4H, CH_2–CH_2–C=O), 4.4–4.6 (m, 4H, benzylic CH_2), 7.26 (m, 4H, Ar–H), 9.77 (s, 2H, Ar–CHO), 9.86 (s, 2H, CH_2–NH). λ_{max}, nm (ε, M^{-1} cm^{-1}) in DMF: 276 (22 450).

2.3.2. Synthesis of 1,8-[N,N-bis(3-formyl-12-hydroxy-5-bromo)-benzyl]-5,12-dioxo-1,4,8,11-tetraazacyclotetradecane (L^2)

Ligand L^2 was prepared by a method similar to that described for L^1 by using 3-chloromethyl-5-bromo salicylaldehyde (1.82 g,

0.008 mol). The crude product thus obtained was recrystallized from acetonitrile to afford L^2 as a yellowish white solid.

Yield: 2.1 g (75 %). M.p: 294 °C. *Anal.* Calc. $C_{26}H_{28}O_6N_4Br_2$: C, 47.87; H, 4.32; N, 8.58. Found: C, 47.80; H, 4.30; N, 8.50%. Selected IR (KBr) (ν/cm^{-1}): 3385 ν(OH), 3294 ν (NH), 1668, 1642 ν(C=O). ^{1}H NMR (δ ppm in $CDCl_3$): 1.9–2.26 (m, 12H, α-CH_2), 3.38–3.43 (m, 4H, CH_2–CH_2–C=O), 4.4–4.8 (m, 4H, benzylic CH_2), 7.26 (m, 4H, Ar–H), 9.77 (s, 2H, Ar–CHO), 9.86 (s, 2H, H_2C–NH–). λ_{max}, nm (ε, M^{-1} cm^{-1}) in DMF: 265 (22 380).

2.3.3. Synthesis of N,N-bis[1,8-dibenzoyl]-5,12-dioxo-1,4,8,11-tetraazacycloteradecane (L^3)

Ligand L^3 was prepared by a method similar to that described for L^1 by using two equivalent of benzoyl chloride (1 mL, 0.009 mol). The crude product thus obtained was recrystallized from DMF to afford L^3 as a white solid.

Yield: 1.24 g (75 %). M.p: 300 °C. *Anal.* Calc. for $[C_{24}H_{28}O_4N_4]$: C, 66.03; H, 6.47; N, 12.83. Found: C, 66.00; H, 6.39; N, 12.76%; Selected IR (KBr) (ν/cm^{-1}): 3295 ν(N–H), 1672, 1634 ν(C=O). ^{1}H NMR (δ ppm in $CDCl_3$): 1.17 (s, 6H, CH_3), 1.9–2.26 (m, 12H, α-CH_2), 3.35–3.43 (m, 4H, CH_2–CH_2–C=O), 7.26 (m, 4H, Ar–H), 9.86 (s, 2H, CH_2–NH). λ_{max}, nm (ε, M^{-1} cm^{-1}) in DMF: 267 (22 410).

2.3.4. Synthesis of N,N-bis[1,8-(2-nitrobenzoyl)]-5,12-dioxo-1,4,8,11-tetraazacyclotetradecane (L^4)

Ligand L^4 was prepared by a method similar to that described for L^1 by using two equivalent of *o*-nitrobenzoyl chloride (1.2 mL, 0.009 mol). The crude product thus obtained was recrystallized from DMF to afford L^4 as a yellowish white solid.

Yield: 1.24 g (65 %) M.p: 280 °C. *Anal.* Calc. for $[C_{24}H_{26}O_8N_6]$: C, 54.74; H, 4.98; N, 15.96. Found: C, 54.63; H, 4.89; N, 15.87%; Selected IR (KBr) (ν/cm^{-1}): 3290 ν(N–H), 1665, 1645, ν(C=O), 1558 $\nu_{asym}(NO_2)$, 1350 $\nu_{sym}(NO_2)$. ^{1}H NMR (δ ppm in $CDCl_3$): 1.17 (s, 6H, CH_3), 1.9–2.26 (m, 12H, α-CH_2), 3.35–3.43 (m, 4H, CH_2–CH_2–C=O), 7.26 (m, 4H, Ar–H), 9.86 (s, 2H, CH_2–NH). λ_{max}, nm (ε, M^{-1} cm^{-1}) in DMF: 280 (22 470).

2.3.5. Synthesis of N,N-bis[1,8-(4-nitrobenzoyl)]-5,12-dioxo-1,4,8,11-tetraazacyclotetradecane (L^5)

Ligand L^4 was prepared by a method similar to that described for L^1 by using two equivalent of *p*-nitrobenzoyl chloride (1.67 g, 0.009 mol). The crude product thus obtained was recrystallized from DMF to afford L^5 as a yellowish white solid.

Yield: 1.24 g (65 %). M.p: 280 °C. *Anal.* Calc. for $[C_{24}H_{26}O_8N_6]$: C, 54.74; H, 4.98; N, 15.96. Found: C, 54.63; H, 4.89; N, 15.87%; Selected IR (KBr) (ν/cm^{-1}): 3275 ν(N–H), 1660, 1642 ν(C=O), 1553 $\nu_{asym}(NO_2)$, 1348 $\nu_{sym}(NO_2)$. ^{1}H NMR (δ ppm in $CDCl_3$): 1.17 (s, 6H, CH_3), 1.9–2.26 (m, 12H, α-CH_2), 3.35–3.43 (m, 4H, CH_2–CH_2–C=O), 7.26 (m, 4H, Ar–H), 9.86 (s, 2H, CH_2–NH). λ_{max}, nm (ε, M^{-1} cm^{-1}) in DMF: 275 (22 450).

2.4. Synthesis of macrocyclic mononuclear copper(II) and nickel(II) complexes

The copper(II) and nickel(II) complexes were prepared by refluxing the respective metal perchlorate (1 mmol) in methanol (50 mL) with appropriate ligands (1 mmol) in DMF (50 mL). The resulting solution was refluxed for 8 h. Then the solution was filtered whilst hot and allowed to stand at room temperature. After the evaporation of solvent, the compound was recrystallised from acetonitrile to get the pure complexes.

2.4.1. [CuL^1]

Brown solid. Yield: 0.89 g (80 %). *Anal.* Calc. for $[C_{28}H_{32}N_4O_6Cu]$: C, 57.55; H, 5.52; N, 9.59, Cu, 10.87. Found: C, 57.50; H, 5.44; N, 9.50, Cu, 10.80%. Selected IR (KBr) (ν/cm^{-1}): 3420 ν(O–H), 1655, 1635 ν(C=O). Conductance (Λ_m/S cm^2 mol^{-1}) in CH_3CN: 18. λ_{max}, nm (ε, M^{-1} cm^{-1}) in DMF: 476 (144), 377 (16 342), 310 (23 620). g_{ll} 2.47, $g_{\perp}$ 2.16, A_{ll} 162. μ_{eff}: 1.70.

2.4.2. [CuL^2]

Brown solid. Yield: 0.76 g (70%). *Anal.* Calc. for $[C_{26}H_{28}N_4O_6Br_2Cu]$: C, 43.74; H, 3.66; N, 7.84; Cu, 8.89. Found: C, 43.67; H, 3.60; N, 7.79, Cu, 8.78%. Selected IR (KBr) (ν/cm^{-1}): 3390 ν(O–H), 1658, 1636 ν(C=O). FAB Mass [M]$^+$: 712. Conductance (Λ_m/S cm^2 mol^{-1}) in CH_3CN: 14. λ_{max}, nm (ε, M^{-1} cm^{-1}) in DMF: 568 (169), 395 (15 400), 312 (33 600). g_{ll} 2.31, $g_{\perp}$ 2.09, A_{ll} 160. μ_{eff}: 1.73.

2.4.3. [CuL^3]

Brown solid. Yield: 0.89 g (80%). *Anal.* Calc. for $[C_{24}H_{26}N_4O_4Cu]$: C, 57.87; H, 5.26; N, 11.24, Cu, 12.75. Found: C, 57.80; H, 5.21; N, 11.19, Cu, 12.69%. Selected IR (KBr) (ν/cm^{-1}): 1659, 1624 ν(C=O). FAB Mass [M]$^+$: 497. Conductance (Λ_m/S cm^2 mol^{-1}) in CH_3CN: 12. λ_{max}, nm (ε, M^{-1} cm^{-1}) in DMF: 490 (145), 380 (12 400), 311 (24 650). g_{ll} 2.30 $g_{\perp}$ 2.07, A_{ll} 171. μ_{eff}: 1.71.

2.4.4. [CuL^4]

Brown solid. Yield: 0.84 g (75%). *Anal.* Calc. for $[C_{24}H_{24}N_6O_8Cu]$: C, 49.01; H, 4.11; N, 14.29, Cu, 10.81. Found: C, 48.97; H, 4.05; N, 14.19, Cu, 10.75%. Selected IR (KBr) (ν/cm^{-1}): 1663, 1639 ν(C=O), 1550 $\nu_{asym}(NO_2)$, 1344 $\nu_{sym}(NO_2)$. Conductance (Λ_m/S cm^2 mol^{-1}) in CH_3CN: 18. λ_{max}, nm (ε, M^{-1} cm^{-1}) in DMF: 538 (162), 392 (14 230), 304 (30 220). g_{ll} 2.29, $g_{\perp}$ 2.09, A_{ll} 170. μ_{eff}: 1.72.

2.4.5. [CuL^5]

Brown solid. Yield: 0.84 g (75%). *Anal.* Calc. for $[C_{24}H_{24}N_6O_8Cu]$: C, 49.01; H, 4.11; N, 14.29, Cu, 10.20. Found: C, 48.97; H, 4.05; N, 14.19, Cu, 10.15%. Selected IR (KBr) (ν/cm^{-1}): 1660, 1639 ν(C=O), 1542 $\nu_{asym}(NO_2)$, 1341 $\nu_{sym}(NO_2)$. Conductance (Λ_m/S cm^2 mol^{-1}) in CH_3CN: 18. λ_{max}, nm (ε, M^{-1} cm^{-1}) in DMF: 542 (160), 387 (14 200), 309 (30 100). g_{ll} 2.31, $g_{\perp}$ 2.10, A_{ll} 162. μ_{eff}: 1.71.

2.4.6. [NiL^1]

Yellowish green solid. Yield: 0.830 g (75%). *Anal.* Calc. for $[C_{28}H_{32}N_4O_6Ni]$: C, 58.03; H, 5.56; N, 9.67, Ni, 10.13. Found: C, 58.00; H, 5.46; N, 9.57, Ni, 10.03%. Selected IR (KBr) (ν/cm^{-1}): 3398 ν(O–H), 1658, 1634 ν(C=O). Conductance (Λ_m/S cm^2 mol^{-1}) in CH_3CN: 16. λ_{max}, nm (ε, M^{-1} cm^{-1}) in DMF: 480 (160), 378 (14 765), 314 (26 600).

2.4.7. [NiL^2]

Yellowish green solid. Yield: 0.86 g (80%). *Anal.* Calc. for $[C_{26}H_{26}N_4O_6Br_2Ni]$: C, 44.04; H, 3.69; N, 7.90, Ni, 8.27. Found: C, 44.00; H, 3.62; N, 7.85; Ni, 8.20%. Selected IR (KBr) (ν/cm^{-1}): 3410 ν(O–H), 1650, 1630 ν(C=O). FAB Mass [M−L]: 708. Conductance (Λ_m/S cm^2 mol^{-1}) in CH_3CN: 13. λ_{max}, nm (ε, M^{-1} cm^{-1}) in DMF: 490 (162), 391 (16 620), 309 (30 280).

2.4.8. [NiL^3]

Yellowish green solid. Yield: 0.73 g (65%). *Anal.* Calc. for $[C_{24}H_{26}N_4O_4Ni]$: C, 58.44; H, 5.32; N, 11.35, Ni, 10.85. Found: C, 58.39; H, 5.27; N, 11.30, Ni, 10.78%. Selected IR (KBr) (ν/cm^{-1}): 1659, 1628 ν(C=O). Conductance (Λ_m/S cm^2 mol^{-1}) in CH_3CN: 15. λ_{max}, nm (ε, M^{-1} cm^{-1}) in DMF: 561 (172), 370 (13 480), 312 (26 600).

2.4.9. [NiL^4]

Yellowish green solid. Yield: 0.80 g (70%). *Anal.* Calc. for $[C_{24}H_{24}N_6O_8Ni]$: C, 49.42; H, 4.15; N, 14.41, Ni, 10.06. Found: C, 49.38; H, 4.05; N, 14.35; Ni, 10.00%. Selected IR (KBr) (ν/cm^{-1}): 1652, 1634 ν(C=O), 1554 $\nu_{asym}(NO_2)$, 1340 $\nu_{sym}(NO_2)$. Conductance

(Λ_m/S cm^2 mol^{-1}) in CH_3CN: 13. λ_{max}, nm (ε, M^{-1} cm^{-1}) in DMF: 520 (145), 380 (16 800), 325 (29 400).

2.4.10. [NiL^5]

Yellowish green solid. Yield: 0.80 g (70%). *Anal.* Calc. for [$C_{24}H_{24}N_6O_8Ni$]: C, 49.42; H, 14.41; N, 7.84, Ni, 10.06. Found: C, 49.38; H, 14.35; N, 7.79; Ni, 10.00%. Selected IR (KBr) (ν/cm^{-1}): 1660, 1634 ν(C=O), 1534 $\nu_{asym}(NO_2)$, 1335 $\nu_{sym}(NO_2)$. Conductance (Λ_m/S cm^2 mol^{-1}) in CH_3CN: 13. λ_{max}, nm (ε, M^{-1} cm^{-1}) in DMF: 546 (155), 385 (16 740), 320 (28 940).

3. Results and discussion

Tetra N-substituted dioxocyclam based ligands have been synthesized and their mononuclear copper(II) and nickel(II) complexes were prepared as shown in Schemes 1 and 2. The complexes were characterized by spectral studies. Their magnetic, electrochemical, catalytic and antibacterial activities are discussed. The molar conductance values of all the copper(II) and nickel(II) complexes fall in the expected range of 12–18 Λ_m/S cm^{-1} mol^{-1}, which indicates that the complexes are neutral [26].

3.1. The structure of ligand L^1

The ligand L^1, crystallize in the space group $P2_1/n$ by slow evaporation method where chloroform was used as solvent. Fig. 1 shows ORTEP diagram of ligand L^1 at 30% probability level.

The ligand contains half molecule in the asymmetric unit and also two water molecules and two chloride ions. Atom N1 and N1a are in protonated state. The sum of the bond angles around the atom N1(333.57°) shows the sp^3 hybridization and N2 (359.66°) shows the sp^2 hybridization. The molecule is stabilized by O–H···O, N–H···O, N–H···N and C–H···O intramolecular interactions and the crystal packing is stabilized by C–H···C and C–H···O intermolecular interactions.

3.2. Spectral studies

The FT IR spectra of the ligands L^1 and L^2 show a sharp band at around 1670 cm^{-1} due to the presence of –CHO group. The OH group in the ligands shows a broad peak around 3400 cm^{-1}. The IR spectra of the ligands L^3–L^5 shows a band in the region of 1634–1680 cm^{-1} is due to the carbonyl group. A band in the region of 3275–3295 cm^{-1} is due to the presence of –NH group. The N-substituted dioxocyclam ligands L^4 and L^5 show strong absorptions at about 1555 cm^{-1} and 1350 cm^{-1} corresponding to –NO_2 stretching vibrations.

All complexes show a sharp band in the region 1624–1652 cm^{-1}, due to νC=O stretching. All complexes of ligands L^1 and L^2 show a broad peak around 3400 cm^{-1}. This shows that the OH group is not coordinated to the metal. The band at about 3290 cm^{-1} is absent in all the complexes which implies that the secondary (N–H) group in all ligands are deprotonated due to complexation. The mononuclear complexes of the ligands L^4 and L^5 show strong absorptions at around 1550 and 1345 cm^{-1} corresponding to –NO_2 stretching vibrations [27].

The electronic spectral data are given in Table S3. In general, the spectra of dioxocyclam complexes are broader than those of cyclam complexes which may be due to the larger splitting of the low-lying d-orbitals in the system with *trans* arrangement of amide donors. The electronic spectra of all the complexes show one peak in the range of 309–325 nm assigned to the intra ligand transition (π–π^*). An intense peak in the range of 370–395 nm is

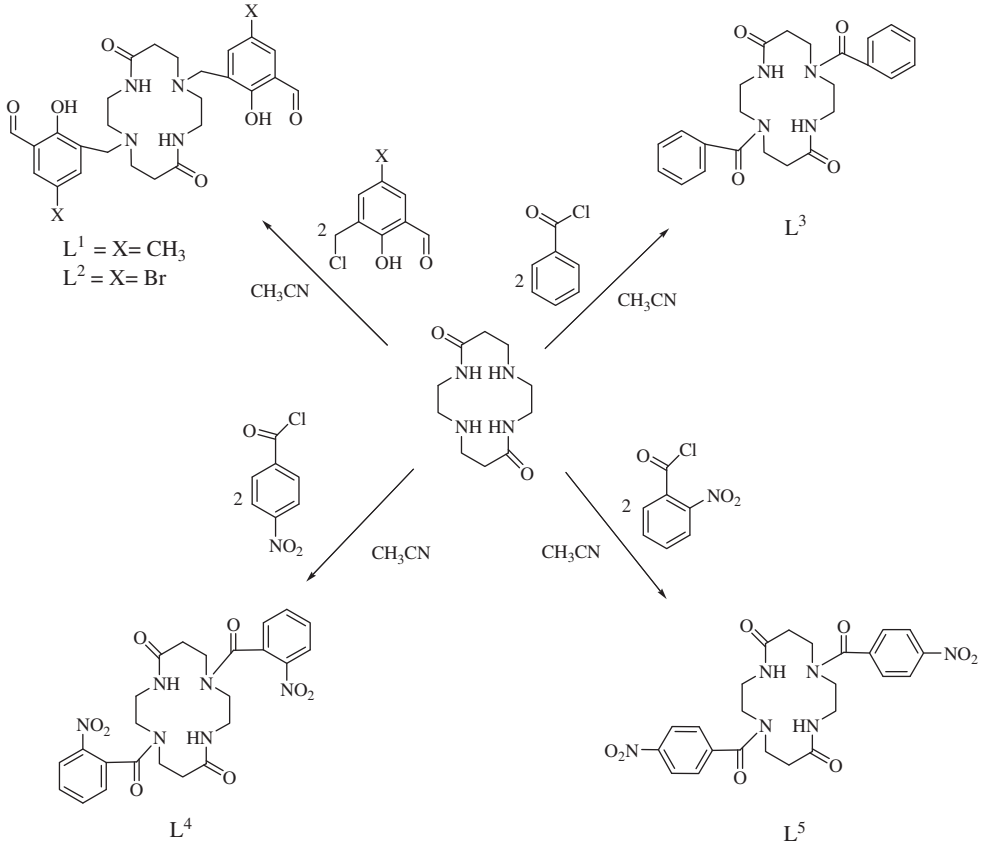

Scheme 1.

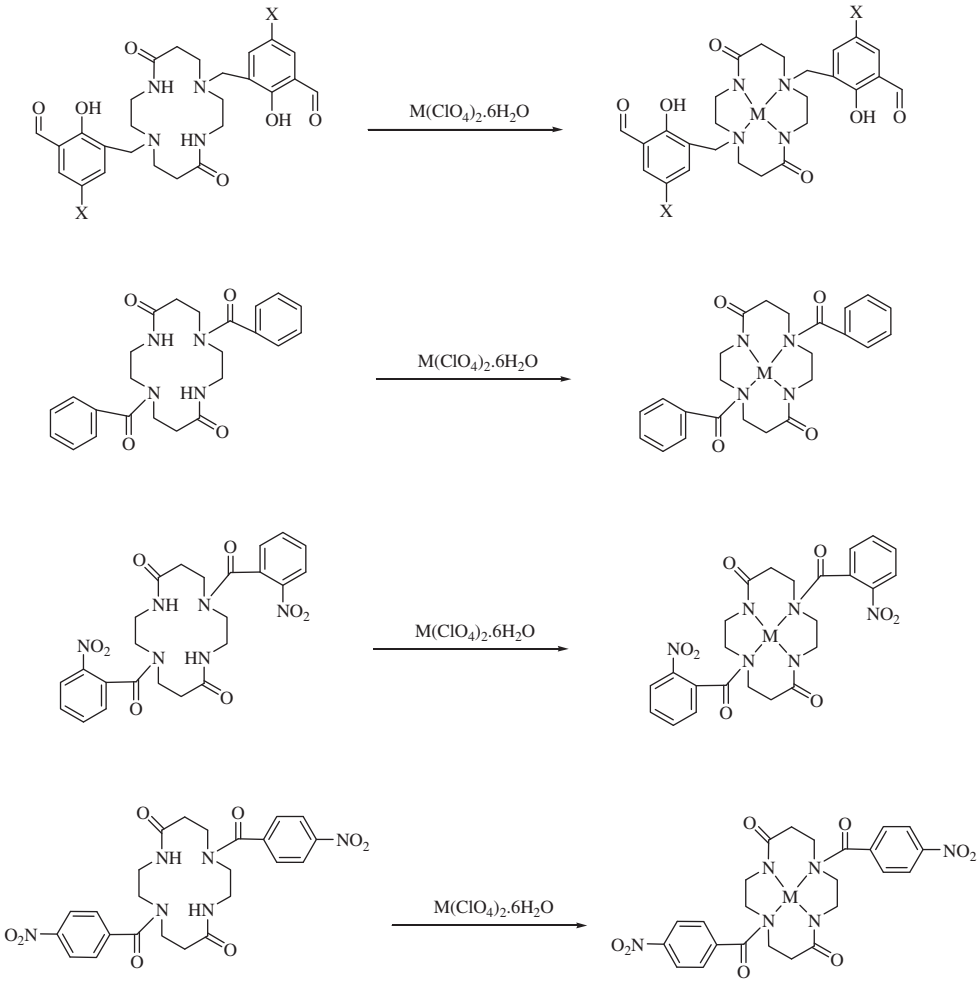

Scheme 2.

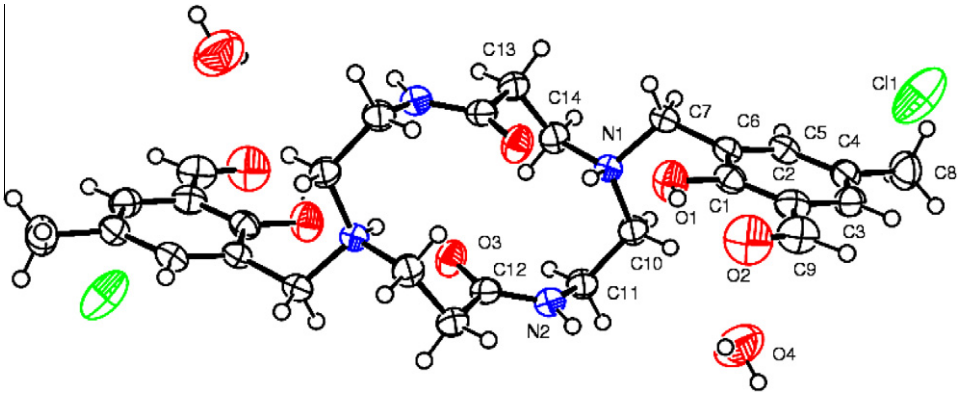

Fig. 1. The ORTEP diagram of the ligand L^1.

due to ligand-to-metal charge transfer transition, and a broad peak in the range of 476–568 nm is due to d–d transitions. The copper(II) complexes show λ_{max} value in the region 476–568 nm is typical for reported square planar tetraazamacrocyclic copper(II) complexes [11,28–30]. The electronic spectra of nickel(II) complexes show a single band in the region 479–520 nm consistent with the transition in a square-planar geometry of the complexes [31–33] with N_4 coordination.

3.3. ESR spectral analysis

The copper(II) complexes show four lines in the ESR spectrum with hyperfine splitting by a nuclear spin of 3/2. The hyperfine A_{II} splitting falls in the range of 160–172 $\times 10^{-4}$ cm^{-1}, indicative of an electron interacting with only one copper nucleus. The relation $g_{II} > g_{\perp}$ is typical of d^9 copper(II) complexes in a ground state doublet with the unpaired electron in a d_{x2-y2} orbital. The g and A_{II}

values of copper(II) complexes are close to the $[Cu(dioxocyclam)]^{2+}$ suggesting essentially square-planar coordination geometry of the mononuclear copper(II) complexes [34–36]. The room temperature (at 298 K) magnetic moment studies of the copper(II) complexes show a μ_{eff} value in the range of 1.70–1.73 BM, which is close to the spin-only value of the copper(II) ion [37]. The nickel(II) complexes are diamagnetic in nature due to square planar geometry around the metal ion [38].

3.4. Electrochemical properties of the complexes

The electrochemical data are summarized in Table S4. The electrochemical properties of the complexes were studied by cyclic voltammetry in dimethylformamide containing 10^{-1} M tetra(*n*-butyl)ammonium perchlorate (TBAP) as supporting electrolyte.

3.4.1. Reduction process at negative potential

The cyclic voltammogram of the copper(II) and nickel(II) complexes were recorded in the potential range 0 to −1.8 V. Cyclic voltammograms for mononuclear $[CuL^1]$ and $[NiL^5]$ complexes are shown in Figs. 2 and 3, respectively. The Cyclic voltammograms show one quasi-reversible reduction wave [39] at negative potential in the range −0.65 to −1.13 V for the complexes derived from L^1, L^2 and L^3. The mononuclear complexes L^4 and L^5 show both metal and ligand (–NO_2) reduction peaks in the cathodic region of −0.78 to −1.07 V and −1.40 to −1.60 V. Among the two reduction peaks the first reduction peak is quasi-reversible and is attributed to the reduction of metal ion in the dioxocyclam compartment, whereas the second reduction is irreversible and corresponds to NO_2 group in the side arm. The ΔE value is always greater than 60 mV. Electrolysis at controlled potential was also carried out and the experiment shows that the couple corresponds to one electron transfer process. Thus, the one electron process occurring at the electrode surface was inferred to be

$$M^{II} \rightleftharpoons M^{I}$$

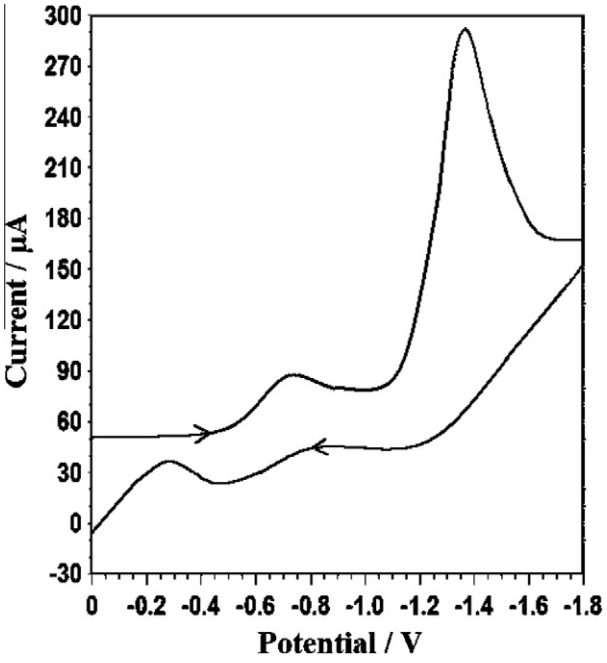

Fig. 3. Cyclic voltammogram of the $[NiL^5]$ complex: (Reduction process).

3.4.2. Oxidation process at positive potential

The cyclic voltammogram for nickel(II) complexes were recorded at anodic potential in the range 0 to +1.6 V. The electrochemical data are summarized in Table S5. The cyclic voltammogram for the nickel(II) complex is shown in Fig. 4. Each voltammogram shows one quasi-reversible oxidation wave [39] at a positive potential in the range +0.95 to +1.06 V. Controlled potential electrolysis indicates that the couple corresponds to one electron transfer process.

$$Ni^{II} \rightleftharpoons Ni^{III}$$

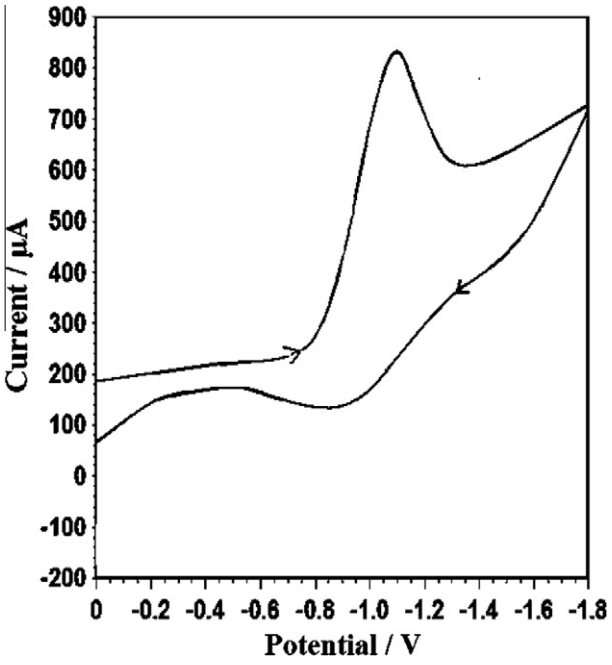

Fig. 2. Cyclic voltammogram of the $[CuL^1]$ complex: (Reduction process).

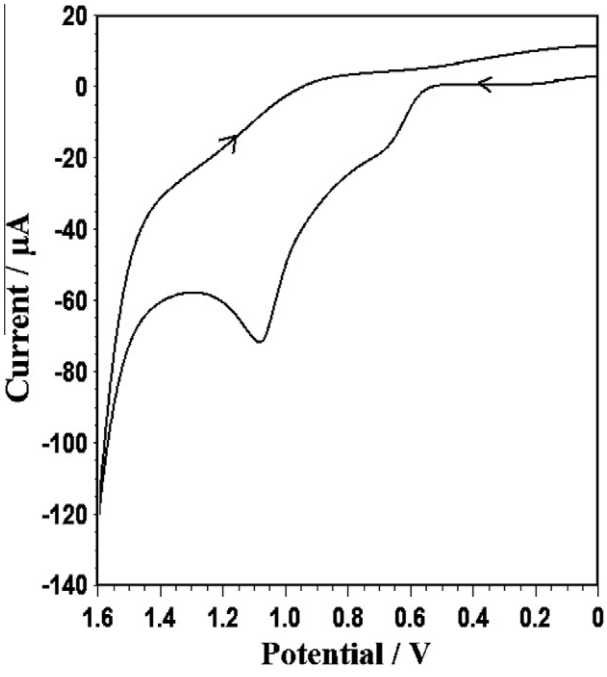

Fig. 4. Cyclic voltammogram of the $[NiL^5]$ complex: (Oxidation process).

3.5. Kinetic studies

3.5.1. Oxidation of pyrocatechol (catecholase activity)

The catecholase activity of the copper(II) complexes was studied using pyrocatechol as a convenient model substrate for the identification of functional models for the metalloenzymes by following the reported methods [40,41]. Solutions (10^{-3} mol dm^{-3}) of complexes in dimethylformamide were treated with 100 equivalents of pyrocatechol in the presence of air. The reaction was followed every 5 min spectrophotometrically at 390 nm for 45 min. The slope was determined from initial rates by monitoring the growth of the 390 nm band of the *o*-quinone product. A linear relationship for initial rate and the complex concentration obtained for the copper(II) complexes shows first-order dependence on the complex concentration. Fig. 5 shows the plots of $\log(A_\infty/A_\infty - A_t)$ versus time for catecholase activity of copper(II) complex of the ligands L^3 and L^4. The initial rate constant values are given in Table S6. It is noteworthy that the reactivity of the complexes differs significantly by varying the N-substitution. The catalytic activity of the complexes is in the range of 2.12–4.41 $\times$ 10^{-3} min^{-1}.

3.5.2. Hydrolysis of 4-nitrophenylphosphate

The catalytic activity of the copper(II) and nickel(II) complexes with respect to hydrolysis of 4-nitrophenylphosphate was determined spectrophotometrically by monitoring the increase in the characteristic absorbance of the 4-nitrophenolate anion at 420 nm in dimethylformamide for 45 min at regular time intervals of 5 min. For this purpose, 10^{-3} mol dm^{-3} solutions of complexes were treated with 100 equivalents of 4-nitrophenylphosphate in the presence of air. A linear relationship for all the complexes shows a first-order dependence on the complex concentration. Fig. 6 shows the results for hydrolysis of 4-nitrophenylphosphate by copper(II) and nickel(II) complexes of the ligand L^2. The observed initial rate constants for the complexes are given in Table S6. The catalytic activity of the complexes is in the range of 1.98–3.92 $\times$ 10^{-3} min^{-1}. The complexes of the ligand L^1 show lower rate constant value than the complexes of L^{2-5}.

The structural features and electrochemical properties are important factors in determining the catalytic activity of the complexes. The catalytic activity of the complex containing electron withdrawing group is higher than that of the complex containing no electron withdrawing group. It can be seen that if the reduction potential is too negative, the complex has a decreased catalytic activity due to a more difficult reduction to metal(I). Literature reports, [42,43] also show that the complexes containing electron-withdrawing groups show higher catalytic activity than complexes with electron donating substituents.

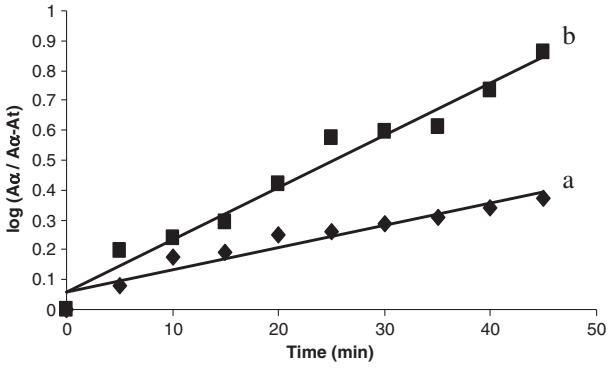

Fig. 5. Catecholase activity by the (a) [CuL^3] (b) [CuL^4] complexes.

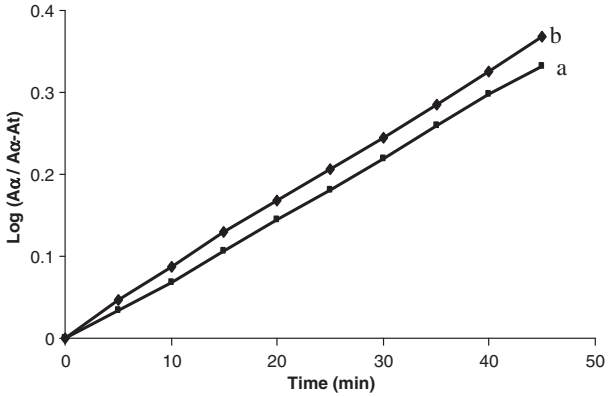

Fig. 6. Hydrolysis of 4-nitrophenylphosphate by (a) [CuL^2] (b) [NiL^2] complexes.

3.6. Antifungal and antimicrobial activities

Antifungal and antibacterial activities of the complexes were tested by the well diffusion method using Sabouraud dextrose agar and Muller Hinton agar [44]. The radial growth of the colony was recorded on completion of the incubation, and the mean diameter for each complex at a concentration of 100 μg/ml was recorded. The average percentage inhibition of the bacterial growth medium was compared using the Vincent equation: $I = 100\,(C - T)/C$, where I = percentage inhibition, T = average diameter of the bacterial growth on the tested plates and C = average diameter of the growth on the control plates. The diameters of the zone of inhibition produced by the compounds were compared with the standard antibiotics Streptomycin 10 μg/well and Azithromycin 15 μg/well (for *Candida albicans*).

3.6.1. Inoculum preparation

Fresh bacterial cultures were used for the antibacterial susceptibility test. Five ATCC colonies of the strains were inoculated to Tryptic soy or Brain Heart Infusion broth and incubated at 37 °C for 22–24 h time period. Turbidity was adjusted with sterile broth so as to correspond to the 0.5 Mc Farland standard, a standard inoculum of the microorganism 1.5 $\times$ 10^6 colony forming units CFU/ml, a 1:100 dilution of a suspension of turbidity equal to a Mc Farland standard 0.5. The turbidity was adjusted to match a Mc Farland 0.5 barium sulfate method. This is prepared by adding 0.5 ml of 1.175% w/v (0.048 m) hydrate ($BaCl_2{\cdot}2H_2O$) to 99.5 ml of 1% w/v (0.36) sulfuric acid.

3.6.2. Antifungal activity

We have evaluated the antifungal activity of all the ligands and metal complexes against the human pathogenic fungus *C. albicans*. The screening data are reported in *Table S7*. The activity observed for the present complexes was comparable with the N-substituted tetraazamacrocycles reported in literature [45]. The copper(II) and nickel(II) complexes show higher activity than their corresponding ligands. Another interesting result observed in this study is that mononuclear complexes of the ligands containing electron withdrawing group show higher activity than the other complexes. It seems from the results that the nature of the ligand and the coordinated metal ion plays a significant role in the inhibition activity.

3.6.3. Antibacterial activity

All the prepared complexes have been screened for their *in vitro* antibacterial activity against selected five pathogenic bacteria such as *Pseudomonas aeruginosa* (ATCC 10145), *Staphylococcus aureus* (ATCC 12600), *Escherichia coli* (ATCC 11775), *Bacillus subtilis* (ATCC 6633), *and Klebsiella pneumonia* (ATCC 13883), respectively. The

screening results are shown in Table S7. All the copper(II) and nickel(II) complexes show comparable activity against all bacteria. The higher activity of the complexes may be ascribed to Tweedy's theory, according to which chelation reduces the polarity of the central metal atom because of partial sharing of its positive charge with the ligand, which favors permeation of the complexes through the lipid layer of the membrane [46]. Further, the extent of inhibition by the complexes depends on the particular type of macrocyclic ligand and the axial ligand/counter ion (perchlorate).

The presence of cyclam unit in the complexes does apparently improve the activity of the complexes. A similar observation holds for copper(II) and nickel(II) complexes of cyclam ligands, as compared to the corresponding complexes with ON donor ligands [47], suggesting that cyclam plays a critical role in activity enhancement. An additional important feature in the biologically active metal complexes of the present investigation may be imparted by the peculiar nature of the ligand in which different cyclam units bring about a change in the coordinating ability. The binding of the complexed metals to the nitrogen bases of the enzymes have been suggested as possible mechanisms of action by earlier workers [47]. The action of these complexes could be due to the interaction of the nucleic acid component of the bacteria with the nitrogen donor ligands (which contains lone pairs) or the d-metal ions which act as good acceptors.

4. Conclusion

Various N-substituted 14-membered macrocyclic dioxocyclams and their copper(II) and nickel(II) complexes have been synthesized. The electronic spectra of Cu(II) and Ni(II) complexes indicate a square planar geometry around the metal ion and cyclic voltammetry of the complexes exhibit one electron quasi-reversible process. Antimicrobial activities have been conducted against five selected pathogenic bacteria and one fungus. All these studies of the complexes agree well with the established trend.

Acknowledgements

The authors are grateful for the financial supports from the University Grants Commission and Council of Scientific and Industrial Research, New Delhi, India.

Appendix A. Supplementary data

CCDC 723256 contains the supplementary crystallographic data for ligand L^1. These data can be obtained free of charge via http://www.ccdc.cam.ac.uk/conts/retrieving.html, or from the Cambridge Crystallographic Data Centre, 12 Union Road, Cambridge CB2 1EZ, UK; fax: (+44) 1223-336-033; or e-mail: deposit@ccdc.cam.ac.uk. Supplementary data associated with this article can be found, in the online version, at doi:10.1016/j.poly.2010.09.036.

References

[1] F.P. Hinz, D.W. Margerum, J. Am. Chem. Soc. 96 (1974) 4993.
[2] E. Kimura, M. Haruta, T. Koike, M. Shionoya, K. Takenouchi, Y. Iitaka, Inorg. Chem. 32 (1993) 2779.
[3] F. Cuenot, M. Meyer, E. Espinosa, A. Bucaille, R. Burgat, R. Guilard, C. Marichal-Westric, Eur. J. Inorg. Chem. (2008) 267.
[4] M. Shokeen, C. Anderson, Acc. Chem. Res. 42 (2009) 832.
[5] S. Wang, T.D. Westmoreland, Inorg. Chem. 48 (2009) 719.
[6] E. Kimura, T. Koike, R. Machida, R. Nagai, M. Kodama, Inorg. Chem. 23 (1984) 4181.
[7] V.J. Thoem, J.C.A. Boeyens, G.J. McDougall, R.D. Hancock, J. Am. Chem. Soc. 106 (1984) 3198.
[8] S. Zhu, F. Kou, H. Lin, C. Lin, M. Lin, Y. Chen, Inorg. Chem. 35 (1996) 5851.
[9] Y.D. Lampeka, S.P. Gavrish, J. Coord. Chem. 21 (1990) 351.
[10] F. Kou, S. Zhu, H. Lin, Y. Chen, H. Wang, X. Yao, Chem. Commun. (1996) 59.
[11] D. Meyerstein, Coord. Chem. Rev. 185–186 (1999) 141.
[12] F. Boschetti, F. Denat, E. Espinosa, A. Tabard, Y. Dory, R. Guilard, J. Org. Chem. 70 (2005) 7042.
[13] E. Kimura, Tetrahedron 48 (1992) 6175.
[14] X.H. Bu, Y.T. Chen, M. Shionoya, E. Kimura, Polyhedron 13 (1994) 325.
[15] X.H. Bu, X.C. Cao, D.L. An, R.H. Zhang, C. Thomas, E. Kimura, J. Chem. Soc., Dalton Trans. (1998) 433.
[16] S. Develay, R. Tripier, F. Chuburu, M.L. Baccon, H. Handel, Eur. J. Org. Chem. (2003) 3047.
[17] A. Gasnier, G. Royal, P. Terech, Langmuir 25 (2009) 8751.
[18] A. Gasnier, J.-M. Barbe, C. Bucher, C. Duboc, J.-C. Moutet, E. Saint-Aman, P. Terech, G. Royal, Inorg. Chem. 49 (2010) 2592.
[19] T.R. Wagler, Y. Fang, C.J. Burrows, J. Org. Chem. 54 (1989) 1584.
[20] X.H. Bu, D.L. An, Y.T. Chen, M. Shionoya, E. Kimura, J. Chem. Soc., Dalton Trans. (1995) 2289.
[21] A. Gasnier, J.-M. Barbe, C. Bucher, F. Denat, J.-C. Moutet, E.S. Aman, P. Terech, G. Royal, Inorg. Chem. 47 (2008) 1862.
[22] SMART (control) and SAINT (integration) Software, Bruker AXS Inc., Madison, Wisconsin, USA, 2001.
[23] G.M. Sheldrick, SHELXS-97 and SHELXL-97, University of Göttingen, Göttingen, Germany, 1997.
[24] L. Frémond, E. Espinosa, M. Meyer, F. Denat, R. Guilard, V. Huch, M. Veith, New J. Chem. 24 (2000) 959.
[25] J.C. Duff, J. Chem. Soc. (1941) 547.
[26] W.J. Geary, Coord. Chem. Rev. 7 (1971) 81.
[27] S. Supriya, A. Raghavan, V.R. Vijayaraghavan, J. Subramanian, Polyhedron 26 (2007) 3388.
[28] M. Hediger, T.A. Kaden, Helv. Chim. Acta 66 (1983) 861.
[29] L. Fabbrizzi, L. Montagna, A. Poggi, T.A. Kaden, L.C. Siegfried, J. Chem. Soc., Dalton Trans. (1987) 2631.
[30] J. Chapman, G. Ferguson, J.F. Gallagher, M.C. Jennings, D. Parker, J. Chem. Soc., Dalton Trans. (1992) 345.
[31] A.B.P. Lever, Inorganic Electronic Spectroscopy, second ed., Elsevier, Amsterdam, 1984.
[32] G. Golub, H. Cohen, P. Paoletti, A. Bencini, L. Messori, I. Bertini, D. Meyerstein, J. Am. Chem. Soc. 117 (1995) 8353.
[33] S.J. Brudenell, L. Spiccia, A.M. Bond, P.C. Mahon, D.C.R. Hockless, J. Chem. Soc., Dalton Trans. (1998) 3919.
[34] S.V. Rasokha, Y.D. Lampeka, I.M. Maloshtan, J. Chem. Soc., Dalton Trans. (1993) 631.
[35] M. Lachkar, G. Guilard, A. Atmani, A. De Cian, J. Fischer, R. Weiss, Inorg. Chem. 37 (1998) 1575.
[36] J. Gradinaru, A. Forni, Y. Simonov, M. Popovici, S. Zecchin, M. Gdaniec, D.E. Fenton, Inorg. Chim. Acta 357 (2004) 2728.
[37] J.D. Crane, D.E. Fenton, J.M. Latour, A.J. Smith, J. Chem. Soc., Dalton Trans. (1991) 2279.
[38] B. Bosnich, M.L. Tobe, G.A. Webb, Inorg. Chem. 4 (1965) 1109.
[39] X.H. Bu, Z.H. Zhang, X.C. Cao, Z.A. Zhu, Y.T. Chen, Transition Met. Chem. 22 (1997) 1.
[40] K. Moore, G.S. Vigee, Inorg. Chim. Acta 66 (1982) 125.
[41] D. Bolus, G.S. Vigee, Inorg. Chim. Acta 67 (1982) 19.
[42] M.J. Mac Lachlan, M.K. Park, L.K. Thompson, Inorg. Chem. 35 (1996) 5492.
[43] M. Rajasekar, S. Sreedaran, R. Prabu, V. Narayanan, R. Jegadeesh, N. Raaman, A. Kalilur Rahiman, J. Coord. Chem. 63 (2010) 136.
[44] S. Magaldi, S. Mata-Essayag, C.H. de Capriles, C. Perez, M.T. Colella, C. Olaizola, Y. Ontiveros, Int. J. Infectious Dis. 8 (2004) 39.
[45] T.G. Roy, S.K.S. Hazari, B.K. Dey, H.A. Miah, C. Bader, D. Rehder, Eur. J. Inorg. Chem. (2004) 4115.
[46] B.G. Tweedy, Phytopathology 55 (1964) 910.
[47] M.R. Maurya, S. Khurana, Shailendra, A. Azam, W. Zhang, D. Rehder, Eur. J. Inorg. Chem. 1 (2003) 1966.